

# Navigating the Noise: A CBF Approach for Nonlinear Control with Integral Constraints

Idris Seidu and Roberto Tron

**Abstract**—Many physical phenomena involving mobile agents involve time-varying scalar fields, e.g., quadrotors that emit noise. As a consequence, agents can influence and can be influenced by various environmental factors such as noise. This paper delves into the challenges of controlling such agents, focusing on scenarios where we would like to prevent excessive accumulation of some quantity over select regions and extended trajectories. We use quadrotors that emit noise as a primary example, to regulate the trajectory of such agents in the presence of obstacles and noise emitted by the aerial vehicles themselves. First, we consider constraints that are defined over accumulated quantities, i.e functionals of the entire trajectory, as opposed to those that depend solely on the current state as in traditional Higher order Control Barrier Functions (HOCBF). Second, we propose a method to extend constraints from individual points to lines and sets by using efficient over-approximations. The efficacy of the implemented strategies is verified using simulations. Although we use quadrotors as an example, the same principles can equally apply to other scenarios, such as light emission microscopy or vehicle pollution dispersion. The technical contribution of this paper is twofold.

## I. INTRODUCTION

Quadrotors have become a transformative force in multiple sectors, including transportation, surveillance, and aerial mapping, revolutionizing the way we approach these fields. However, one critical challenge facing quadrotors, and serving as a potential barrier to their broader acceptance in urban environments, is the noise they emit.

In order to overcome these challenges, this work explores the application of Control Barrier Functions (CBFs) for the navigation and control of agents (quadrotor). CBFs have proven to be an effective tool in the design of controllers for real-time collision avoidance with safety guarantees in nonlinear systems [1].

The foundational work by [1] demonstrates how CBFs can be combined with Control Lyapunov Functions (CLFs) using Quadratic Programs (QPs), providing a robust framework for ensuring the forward-invariance of a set with conditions that are linear in the inputs, hence facilitating their use as QPs. CBFs find common application in safety-critical systems, particularly when used alongside CLFs (e.g., adaptive cruise control scenarios [1], [2]). Beyond this, CBFs have been applied to multi-robot systems, illustrating their versatility. For instance, [3] and subsequent extensions in [8], [9] have showcased the application of safety barrier certificates in ensuring collision-free interactions among robots.

This work was supported by a grant from NASA. Idris Seidu and Roberto Tron are with the Department of Mechanical Engineering, Boston University, 110 Cummington Mall, MA 02215, United States tron@bu.edu, idriseid@bu.edu

In another line of work for safety-critical control of quadrotors, CBFs have been integrated with geometric control [10], [11]. These works, as the majority of the literature, have considered CBFs that are defined on the value of a single, current state of the system. In the type of applications considered in this paper, however, we are interested in constraints that depend on the *entire* trajectory of the system (including past states).

Another significant body of work has focused on the application of CBFs over time-varying sets. For instance, [7] introduces a time-varying CBF for nonautonomous control-affine systems, addressing time-dependent safety constraint problems and introducing a control law assisted by humans. Again, however, the applicability of such approaches is limited in scenarios where the definition of the set does not depend on past states of the system.

In parallel, [6], [13] proposed frameworks and planners based on Signal Temporal Logic and time-varying CBFs. These contributions are crucial for the development of computationally efficient control methods under temporal logic tasks, especially in multi-robot systems. However, while these works discuss spatio-temporal constraints over entire trajectories, they do not address the type of constraints based on the accumulation of a scalar field at specific locations.

With respect to the state of the art reviewed above, our paper provides the following main contributions.

- We introduce the use of constraints based on integral cost functionals that track an accumulated cost  $J(x, t)$  at specific locations  $x$  over time  $t$ . While we rely on existing HOCBF theory, its application to constraints of the form  $J(x, t) \leq J_{\text{limit}}$ , where  $J$  is a trajectory-dependent integral, is novel.
- We introduce a method that saves on computational effort by over-approximating constraints across lines and dense sets, rather than individual points. By setting a Control Barrier Function (CBF) on an upper bound  $\bar{J} > J_{\text{max}}$ , where  $J_{\text{max}}$  is the theoretical maximum value of  $J$  over a set, we avoid the need to constantly track  $J_{\text{max}}$ , significantly reducing computational demands.

Together, these contribution allow us to control mobile agents such as quadrotors on paths that are not only void of collisions, but also enforce limits on the accumulation of a scalar field such as noise. It's important to note that while this paper primarily focuses on quadrotors as an example of mobile agents emitting noise, the underlying principles of our approach have broader applications. These principles can be equally applied to scenarios such as managing light emission

in microscopy to minimize sample bleaching, or controlling vehicle pollution dispersion in an urban environments.

## II. PRELIMINARIES

Consider the following nonlinear control-affine system:

$$\dot{x} = f(x) + g(x)u \quad (1)$$

where  $x \in \mathbb{R}^n$  is the system state and  $u \in \mathbb{R}^m$  is the control input while  $f(x)$  and  $g(x)$  are the smooth vector fields. The  $\nabla$  operator represents the gradient for scalar-valued functions that are differentiable with respect to  $x$ . Additionally, the time derivative of a function  $h(x(t))$  with respect to time  $t$  is denoted as  $\dot{h}(x) = \frac{d}{dt}h(x(t))$ . The Lie derivative  $L_f h = \nabla h^T f$  measure the changes in a function  $h$  along the vector field(s)  $f$ .

*Definition 1 (Time-Varying Control Barrier Functions):*

A function  $h(x, t)$  is a Time-Varying Control Barrier Function (TV-CBF) for the system (1) if, for all  $x \in \mathbb{R}^n$  and  $t \geq 0$ , it satisfies:

$$\sup_{u \in \mathbb{R}^m} \left[ L_f h(x, t) + L_g h(x, t)u + \frac{\partial h}{\partial t}(x, t) \right] \geq -\alpha(h(x, t)) \quad (2)$$

A TV-CBF reduces to a regular CBF if  $h$  is constant with respect to time.

The concept of Higher Order Control Barrier Functions (HOCBFs) extends traditional barrier functions to accommodate systems where safety constraints are dependent on higher-order derivatives of the system state. This extension is necessary for systems where the control does not directly influence lower-order derivatives. This concept is made more rigorous with the following.

*Definition 2 (Relative degree):* The relative degree of a sufficiently differentiable function  $h : \mathbb{R}^n \rightarrow \mathbb{R}$  with respect to the dynamics (1) is defined as the number of Lie derivatives needed until the control input  $u$  explicitly appears.

*Definition 3 (Higher Order Barrier Functions):* For a function  $h : \mathbb{R}^n \times [t_0, \infty) \rightarrow \mathbb{R}$  that is differentiable up to order  $m$ , we construct a sequence of functionals  $\Phi_0, \Phi_1, \dots, \Phi_m$ , where  $\Phi_i : \mathbb{R}^n \times [t_0, \infty) \rightarrow \mathbb{R}$  for  $i \in \{0, \dots, m\}$ , specified by:

$$\Phi_0(x, t) := h(x, t), \quad (3)$$

$$\Phi_i(x, t) := \dot{\Phi}_{i-1}(x, t) + \alpha_i(\Phi_{i-1}(x, t)), \quad \text{for } i = 1, \dots, m, \quad (4)$$

with each  $\alpha_i$  being a class  $\mathcal{K}$  function.

Correspondingly, we associate a collection of sets  $B_i(t)$  for  $i \in \{1, \dots, m\}$ , defined as:

$$B_i(t) := \{x \in \mathbb{R}^n : \Phi_{i-1}(x, t) \geq 0\}. \quad (5)$$

*Definition 4 (Higher Order Control Barrier Functions):*

Consider the sets  $B_1(t), \dots, B_m(t)$  established by the preceding definition, along with their associated functions  $\Phi_0, \dots, \Phi_m$ . A function  $h : \mathbb{R}^n \times [t_0, \infty) \rightarrow \mathbb{R}$  is a High-Order Control Barrier Function (HOCBF) with relative degree  $m$  for the given system 1 if there exist differentiable

class  $\mathcal{K}$  functions  $\alpha_1, \dots, \alpha_m$  and control input  $u$  that satisfy:

$$L_f^m h(x, t) + L_g L_f^{m-1} h(x, t)u + \frac{\partial^m h(x, t)}{\partial t^m} + G(h(x, t)) + \alpha_m(\Phi_{m-1}(x, t)) \geq 0, \quad (6)$$

for all  $(x, t) \in B_1(t) \cap B_2(t) \cap \dots \cap B_m(t) \times [t_0, \infty)$

. The equation above involves  $G(h(x, t))$  which represents the remaining Lie derivatives along  $f$  and partial derivatives with respect to  $t$  that have a degree equal to or lower than  $m - 1$  as discussed in [12].

*Theorem 1:* From the HOCBF given in Definition 4 with its related sets  $B_1(t), B_2(t), \dots, B_m(t)$  defined in (5), if  $x(t_0) \in B_1(t_0) \cap B_2(t_0) \cap \dots \cap B_m(t_0)$ , then any Lipschitz continuous controller  $u(t) \in \mathcal{U}$  that satisfies (6) for all  $t \geq t_0$  renders the sets  $B_1(t), B_2(t), \dots, B_m(t)$  forward invariant for system (1).

## III. CBF OVER TIME INTEGRALS

In this section, we extend the traditional CBF formulation to encompass constraints that are based on the accumulated effect over time, rather than relying solely on instantaneous state values. Let  $x(t)$  be the trajectory of an agent, and  $p(q; x)$  be a scalar field function  $\mathbb{R}^d \rightarrow \mathbb{R}_+$  representing the effect of the agent at each point  $q$  when the agent is at location  $x$ . We define an integral cost functional of the form:

$$J(q, t) = \int_0^t p(q, x(\tau)) d\tau, \quad (7)$$

which is a functional representing the cumulative effect at a given location  $q$ .

*Problem 1:* Given a set  $\mathcal{Q} \subseteq \mathbb{R}^d$ , let  $J_{\text{limit}}$  be the maximum permissible value of  $J(q, t)$ . Find constraints on the control input  $u$  for the dynamical system (1) such that the resulting trajectory  $x(t)$  satisfies  $J(q, t) \leq J_{\text{limit}}$  for every time  $t > 0$  and every location  $q \in \mathcal{Q}$ .

We propose to tackle Problem 1 using the following function as a CBF

$$h_J(x, t) = \min_{q \in \mathcal{Q}} (J_{\text{limit}} - J(q, t)). \quad (8)$$

In the following we derive constraints for different types of sets  $\mathcal{Q}$ : single points, line segments, and general polygons. Our analysis primarily focuses on two-dimensional (2-D) spaces, but the same theory could be extended to three-dimensional (3-D) spaces, although we leave this generalization for future research.

### A. Constraint for a single point

If the set  $\mathcal{Q}$  contains a single point,  $\mathcal{Q} = \{q_0\}$ , the Control Barrier Function (8) reduces to:

$$h_J(x, t; q_0) = J_{\text{limit}} - J(q_0, t). \quad (9)$$

Taking derivatives until the control  $u$  appears explicitly we obtain:

$$\dot{h}_J(x, t; q_0) = -p(q_0, x), \quad (10)$$

$$\ddot{h}_J(x, t; q_0) = -\nabla_x p(q_0, x)^T (f(x) + g(x)u); \quad (11)$$

here and for the remainder of the paper, we assume that  $\nabla_x p(q_0, x)^\top g(x) \neq 0$ , which implies that  $h_J$  has relative degree  $m = 2$ . Applying the HOCBF framework reviewed above, we have:

$$\Phi_{J,1}(x, t; q_0) := -p(q, x(t)) + \alpha_1 h_J(x, t) \quad (12)$$

$$\Phi_{J,2}(x, t; q_0) := \dot{\Phi}_{J,1}(x, t) + \alpha_2 \Phi_{J,1}(x, t) \quad (13)$$

The constraint then becomes:

$$\Phi_{J,2}(x, t; q_0) \geq 0 \quad (14)$$

This constraint is linear in  $u$ , and will be incorporated in a Quadratic Program (QP). Overall, this case is a relatively straightforward application of the HOCBF framework, with the only consideration being that the integral in the cumulative cost (7) makes the use of high-order CBFs necessary (i.e., the relative degree is  $m \geq 2$ ) even when the dynamics (1) is first-order.

### B. Constraint for a line segment using upper bounds

This section considers the case where the set  $\mathcal{Q}$  is a line segment with endpoints  $q_0, q_K$ . We use the following parametrization of the set, with  $s \in [0, 1]$ :

$$q(s) = (1 - s)q_0 + sq_K; \quad (15)$$

Ideally, we would like to satisfy the constraint on  $\Phi_{J,2}$  for all the points in the set (i.e., all the values of  $s$ ). However, this leads to having an infinite number of constraints because the parameter  $s$ , which dictates the point's location on the line segment, is a continuous value. An alternative strategy is to keep track of  $s^*$  and  $J_{\max}$  defined by the equation:

$$s^*(t) = \underset{s}{\operatorname{argmax}} J(q(s), t) \quad (16)$$

$$J_{\max}(t; q_0, q_1) = J(q(s^*(t)), t) \quad (17)$$

Note that we employ the max operator (instead of the minimum operator) due to the presence of a negative sign in the minimization of (8).

However, this strategy would require updating  $s^*$ , which also requires keeping track of the full function  $J(q(s), t)$  (which is infinite-dimensional, since it is a continuous function).

In practice, it is necessary to introduce some form of approximation. We consider two strategies: a naïve approximation of the segment with points, and an approximation of the CBF constraint with an upper bound that can be easily updated.

1) *Naïve solution using discretization:* Let  $\bar{\mathcal{Q}} = \{q_k\}_{k=0}^K$  be a discretization of the original set  $\mathcal{Q}$  with  $K$  points. The most naïve way to approximate (8) is to transform it into a series of constraints  $h(x, t; q_k) \geq 0$  for every  $k$  in  $\{0, \dots, K\}$ , where each point  $q_k$  is an element of  $\bar{\mathcal{Q}}$ . We then define a HOCBF constraint

$$\Phi_{J,2}(x, t; q_k) \geq 0 \quad (18)$$

for every  $k$ .

Effectively, this replaces  $\min_{q \in \mathcal{Q}} J(q, t)$  in (8) with  $\min_{q \in \bar{\mathcal{Q}}} J(q, t)$ . This, however, causes two problems: in order to obtain a good approximation, we might need a large number of points (thus incurring in the curse of dimensionality). More importantly, there might always be a point  $q \in \mathcal{Q}$  for which  $J(q, t) > J_{\text{limit}}$ , independently from how fine the discretization is (i.e., independently from the value of  $K$ ). This inherent deficiency prompts the next approach.

2) *Approximation without discretization:* Rather than attempting to track the maximum cumulative effect over  $s$  directly, we propose to compute a bound. Let  $q_0, q_K$  be two consecutive points on the boundary of the region we want to protect from the cumulative noise. We would like to enforce a CBF constraint on  $J_{\max}$  in (17), as that would protect all the points on the line between  $q_0$  and  $q_K$ . However, keeping track of  $J_{\max}$  is computationally costly because we would need to keep track of  $s^*$ , which in turn would require a maximization of  $J(q(s), t)$  (which would require evaluating integrals for the sequence of  $s$  decided by the solver, for every time step).

Instead, we define an upper bound  $\bar{J}$  on  $J_{\max}$  as:

$$\bar{J}(0; q_0, q_K) = J_{\max}(0) \quad (19)$$

$$\dot{\bar{J}}(t; q_0, q_K) = \max_s p(q(s), x(t)). \quad (20)$$

Note that the argument of the maximum in (20) is the kernel  $p$ , not the integral over time. Intuitively, we propose to use  $\bar{J}$  to define a lower bound on (8), and then use this lower bound as a CBF we can enforce safety for every point.

*Proposition 1:* Define the lower-bound CBF

$$h_J(x, t; q_0, q_K) = \min_{q \in \bar{\mathcal{Q}}} (J_{\text{limit}} - \bar{J}(t; q_0, q_K)), \quad (21)$$

and the corresponding HOCBFs functions

$$\bar{\Phi}_1(x, t; q_0, q_K) := -p(q, x(t)) + \alpha_1 h_J(x, t), \quad (22)$$

$$\bar{\Phi}_2(x, t; q_0, q_K) := \dot{\bar{\Phi}}_1(x, t) + \alpha_2 \bar{\Phi}_1(x, t). \quad (23)$$

If the control  $u(t)$  satisfies the HOCBF constraint

$$\bar{\Phi}_2(x, t; q_0, q_K) \geq 0 \quad (24)$$

then  $J_{\max}(t) \leq J_{\text{limit}}$  for all  $t \geq 0$ .

*Proof:* First, from the definition of  $J_{\max}$  in (17) and the fundamental theorem of calculus,

$$\dot{J}_{\max}(t) = p(q(s^*), x(t)). \quad (25)$$

From the definition of  $\bar{J}$  in (20), we have

$$\dot{\bar{J}}(t) = \max_s \dot{J}(t) = \max_s p(q(s), x(t)) \geq \dot{J}_{\max}(t), \quad (26)$$

where the last inequality is given by the fact that the location  $s^*$  where  $J$  is maximum is not necessarily also the one that is currently increasing the most, i.e., where  $\dot{J}$  is maximum.

From 19 and (26), and applying Gronwall's comparison lemma [4] we have (24).

$$J_{\max}(t) \leq \bar{J}(t) \quad (27)$$

for all  $t \geq 0$ . Then, if (24) holds, from Theorem 1 we have

$$J_{\max}(t) \leq \bar{J}(t) \leq J_{\text{limit}}. \quad (28)$$

The claim follows.  $\blacksquare$

### C. Constraints for a general 2-D polygon using upper bounds

Given a polygon  $\mathcal{P}$  defined by vertices  $\{v_1, v_2, \dots, v_N\}$  in  $\mathbb{R}^n$ , the boundary of  $P$  can be defined as a sequence of linear segments  $[v_i, v_{i+1}]$  for  $i = 1, 2, \dots, N$ , with  $v_{N+1} = v_1$  to complete the polygon. We assume the use of a regular CBF to enforce  $x \notin \mathcal{Q}$ . As a result, we can reduce the goal of protecting all segments in  $\mathcal{Q}$  to the goal of protecting the boundary of  $\mathcal{P}$ . we extend the equation (8), where the CBF  $h_J$  is adapted to address the cumulative effect constraints across the polygon's boundary segments. For each segment  $[v_i, v_{i+1}]$ , we can apply the methodology described in Section III-B to define the lower-bound CBF  $h_{\bar{J}}(x, t; v_i, v_{i+1})$  for each segment  $i \in \{1, \dots, N\}$ , which lead to  $N$  HOCBF constraints of the form

$$\bar{\Phi}_2(x, t; v_i, v_{i+1}) \geq 0. \quad (29)$$

Furthermore, to ensure that the agent doesn't pass through this polygon, the obstacle CBF constraint is applied alongside equation 29.

## IV. CASE STUDY

This section outlines a case study focusing on the application of our CBF approach on a simplified model of a quadrotor with first-order-integrator dynamics navigating through a noise-sensitive environment. We consider a simple isotropic distance-based noise model as the scalar field. The goal is then to guarantee that the accumulated noise at any point on a building (modeled as a polygon) is below the desired limit.

### A. Quadrotor model

In our representation, the quadrotor is illustrated as comprising four propellers, represented by four disks, tangent to each other, each with its own center. This arrangement surrounds the quadrotor's central point, which we denote as  $x$ . These individual circles are referred to as "propeller disks", and  $r_{\text{quad}}$  is the radius of each disk.

### B. Obstacle model

The obstacle is represented as a static box and for the purpose of collision avoidance, the quadrotor's proximity to the obstacle is quantified by the position of the nearest propeller disk. Within the context of the quadrotor model,  $x_{\text{quad}}$  is defined as the center of the propeller disk that is closest to the box at any given time. Also,  $x_{\text{box}}$  is defined as the point on the surface of the box that is nearest to the aforementioned propeller disk. These are used to define the CBF for the obstacle.

### C. Application of CBF-QP for obstacles

The dynamics of the quadrotor is modeled as a single integrator  $\dot{x} = u$ . We define the barrier function,  $h_{\text{obs}}(x)$ , as  $h_{\text{obs}}(x) = \|x_{\text{quad}} - x_{\text{box}}\| - r_{\text{quad}}$ . The CBF-QP for the quadrotor becomes

$$\begin{aligned} & \min_u \|u - k_{\text{ref}}(x)\|^2 \\ & \text{subject to } \dot{h}_{\text{obs}}(x) + \alpha_1 h_{\text{obs}}(x) \geq 0 \end{aligned} \quad (30)$$

where  $k_{\text{ref}}(x) = x_{\text{goal}} - x(t)$ .

Herein,  $x(t)$  denotes the quadrotor's position at discrete time intervals, while  $x_{\text{goal}}$  represents the quadrotor's intended destination. An example of this is shown in the simulation section. In the case of multiple obstacles, the CBF-QP can be extended with multiple constraints, each representing a different obstacle. For each obstacle, we can define a barrier function  $h_{\text{obs}}^{(i)}(x)$  where  $i$  is the obstacle index, ensuring that the quadrotor maintains a safe distance from all obstacles. The QP can be augmented to accommodate all these constraints, ensuring a collision-free trajectory even in cluttered environments.

### D. Parabolic kernel noise model

We represent the state-dependent noise scalar field  $p(q, x(\tau))$  for the quadrotor using a parabolic kernel:

$$p(q, x(\tau)) = \begin{cases} A - \sigma \|q - x(\tau)\|^2 & \text{if } \|q - x(\tau)\| \leq \sqrt{\frac{A}{\sigma}} \\ 0 & \text{otherwise} \end{cases} \quad (31)$$

In this formulation,  $A$  represents the peak value of the kernel, indicative of the maximum intensity of the noise (which it a the quadrotor's center). The parameter  $\sigma$  controls the width of the parabola, essentially determining the spread of the kernel. The right hand side  $\sqrt{\frac{A}{\sigma}}$  represents the effective radius within which the kernel possesses non-zero values, marking the boundary of the noise influence. Note that this is a very simplified model, but it captures the fact that the influence of the noise on point  $q$  is nonlinear and state-dependent.

In general, the computation of the bound  $\bar{J}$  requires the maximization of  $p$  (equation (26)). For the case of the parabolic kernel (31) and where the set  $\mathcal{Q}$  is a line parameterized by  $s$ , the optimization problem can be solved in closed form.

*Lemma 1:* Given the parabolic kernel noise model (31) defined over the line segment parameterized by  $s$  with endpoints  $q_0$  and  $q_K$ , the optimization problem is to maximize  $p(q(s), x(\tau))$ . The solution to this optimization problem is:

$$s^* = \frac{(x(\tau) - q_0)^T (q_K - q_0)}{|q_K - q_0|^2}. \quad (32)$$

The maximum corresponds to the point  $q^* \in q_0, q_K$ :

$$q^* = \begin{cases} q_0 & \text{if } s^* < 0 \\ q_K & \text{if } s^* > 0 \\ q(s^*) & \text{otherwise} \end{cases} \quad (33)$$

*Proof:* We first express  $p(q(s), x(t))$  in terms of  $s$ :

$$p_s(q(s), x(t)) = A - \sigma \|(1-s)q_0 + sq_K - x\|^2$$

subject to:

$$\|(1-s)q_0 + sq_K - x(t)\| \leq \sqrt{\frac{A}{\sigma}}$$

We differentiate  $p_s$  with respect to  $s$ :

$$\frac{dp_s}{ds} = -2\sigma((1-s)q_0 + sq_K - x(t))^T (q_K - q_0)$$

Setting this to zero, we get:

$$(q(s) - x(t))^T (q_K - q_0) = 0$$

Solving for  $s$ :

$$\begin{aligned} 0 &= ((1-s)q_0 + sq_K - x(t))^T (q_K - q_0) \\ &= (q_0 - x(t) + (q_K - q_0)s)^T (q_K - q_0) \\ &= (q_K - q_0)^T (q_K - q_0)s + (q_0 - x(t))^T (q_K - q_0), \end{aligned} \quad (34)$$

from which (32) follows.  $\blacksquare$

The value of  $s^*$  is used to determine the optimal point  $q^*$  on the line segment as shown in (33). With  $q^*$  identified, we can now define the barrier function  $\bar{\Phi}_2(x, t; q_0, q_1)$ , which incorporates the noise footprint constraints into the control strategy, ensuring that the cumulative effect at  $q^*$  remains within the specified limits.

$$\begin{aligned} \bar{\Phi}_2(x, t; q_0, q_K) &:= -2\sigma(q - x(t))u \\ + \alpha_2 \left( -(A - \sigma\|q - x(t)\|^2) + \alpha_1 (J_{\text{limit}} - \bar{J}(q, t)) \right) &\geq 0 \end{aligned} \quad (35)$$

Consequently, from (30), the refined Quadratic Programming (QP) formulation is given as:

$$\begin{aligned} \min_u &\|u - k_{\text{ref}}(x)\|^2 \\ \text{s.t.} &\dot{h}_{\text{obs}}(x) + \alpha_1 h_{\text{obs}}(x) \geq 0, \\ &\bar{\Phi}_2(x, t; q_0, q_K) \geq 0. \end{aligned} \quad (36)$$

The solution to (36) (assuming it is feasible) will respect both the obstacle and the noise footprint constraints.

## V. SIMULATION RESULTS

This section details simulation results demonstrating the quadrotor's navigation using CBFs for obstacle avoidance and noise management. We showcase how these strategies enable the quadrotor to safely navigate and comply with environmental constraints, highlighting the practical effectiveness of our control approach.

### A. Simulation parameters

We evaluate our approach with a simulation in an environment with a single obstacle and the simulation is based on Euler's method for integration through time. The focus of the paper is on local control, and a single obstacle allows us to better demonstrate the effect of the various parameters. Navigating more complex environments would require integration with high-level path planning algorithms such as RRT\* [5], which, however, are out of scope for this paper. The following parameters were used for the simulation: the class- $\mathcal{K}$  function for the obstacle CBF and noise CBF constraint uses  $\alpha_1 = 3.0$ ; for the noise CBF constraint, we use  $\alpha_2 = 6.0$ ; the size of the quadrotor is given by  $r_{\text{quad}} = 0.1$ ; the Euler integration time step is  $\delta = 0.1$  s; the obstacle is a square  $\mathcal{Q} = [0, 1] \times [0, 1]$ ; finally, the initial position is  $x(0) = \begin{bmatrix} 3 \\ 3 \end{bmatrix}$ . As the reference controller, we use a simple proportional controller  $k_{\text{ref}}(x) = x_{\text{goal}} - x$ , where  $x_{\text{goal}} = \begin{bmatrix} -2 \\ -1 \end{bmatrix}$ .

### B. Obstacle CBF alone

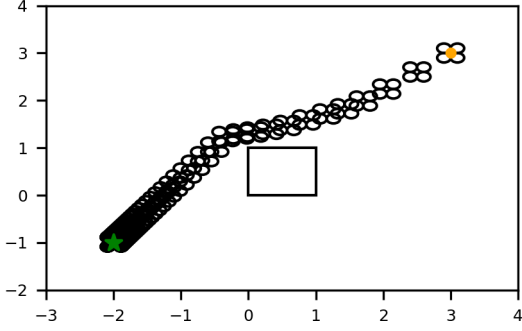
Figure 1a shows the result of the simulation using the QP with only the obstacle CBF constraints (30). In the figure, the trajectory's goal is symbolized by a green star while the starting position is shown in orange, and it is observable that the quadrotor maintains a safe distance from the obstacle towards the goal, adhering to established safety measures. Since this simulation does not take into account the constraint  $J(t) < J_{\text{limit}}$ , while the quadrotor effectively avoids the specified physical obstacles, it may exceed the allowable cumulative impact at certain locations. As seen in Figure 2 the cumulative noise  $J_{\text{obs}}$  exceeded the limit  $J_{\text{limit}}$  for the trajectory.

### C. Cumulative noise CBF with discretization

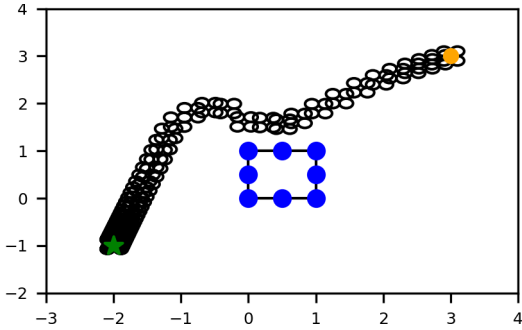
In this section, we show the simulation of the quadrotor with discretization of sets to account for the noise around the obstacle. For this simulation, we used  $J_{\text{limit}} = 0.2$ ,  $A = 0.5$ ,  $\sigma = 0.35$  and  $K = 8$ . Figure 1b shows the result of the simulation, where we use eight constraints obtained by discretizing the boundary of the obstacle and applying individual point-wise constraints as described in Equation (18). Incorporating the noise CBF constraints in the QP formulation, as visualized in Figure 1b, results in a trajectory that is more considerate of the noise impact of the quadrotor compared to the simulation shown in Figure 1a. This is evident from Figure 2, where the cumulative noise  $J_{\text{discr}}(t)$ , representing the cumulative noise subject to the discretized constraints, remains below  $J_{\text{limit}}$ . Also Figure 2 shows the plots of  $J_{\text{max}}(t)$  being below the limit, where  $J_{\text{max}}(t) = \max_{i=0}^{99} J(q_i, t)$  and  $q_0, q_1, \dots, q_{99}$  are the discretized points of the square.

### D. Cumulative noise CBF with bound $\bar{J}$

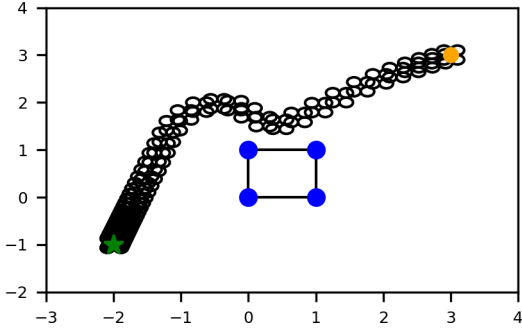
In this section, we share the results of simulations where we applied a Control Barrier Function (CBF) constraint on  $\bar{J}$ . The parameters used are the same as above. Fig. 1c shows the quadrotor navigating toward its goal, detouring upon encountering an obstacle. The escalating noise around this obstacle prompts the quadrotor to maintain distance, thereby steering clear of the accumulating noise while persistently moving toward its target. The difference between this method and the method in Section V-C, is that in the discretization method depicted in Figure 1b, the noise constraints are applied only at specific points along the boundary of the obstacle. This method risks overlooking some areas along the boundary where noise accumulation might exceed the limit, because it does not account for the entirety of the line segment, while in the bound  $\bar{J}$  approach, a CBF constraint is imposed on an over-approximation of the maximum cumulative noise, ensuring that no point along the line segment will exceed the noise threshold which can be seen in Figure 2 as  $\bar{J} < J_{\text{limit}}$ . The corners of the box, are points used to symbolize the segments forming the boundary of the obstacle  $q_0, q_1, q_2$ , and  $q_3$ .



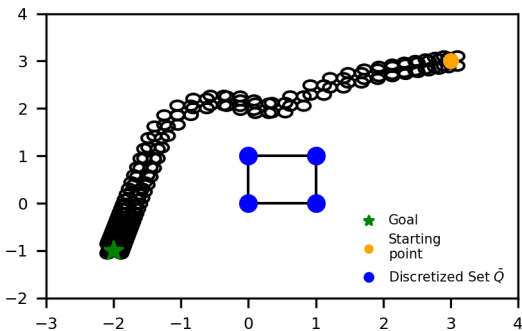
(a) System trajectories for the QP-based control of the quadcopter with box obstacle



(b) Application of Discretization



(c) QP-based control of the quadcopter with noise and obstacles using approximation without discretization



(d) Approximation without discretization with different parameters

Fig. 1: System trajectories with just the obstacle, noise using discretization, noise but with approximation without discretization and approximation without discretization with different parameters

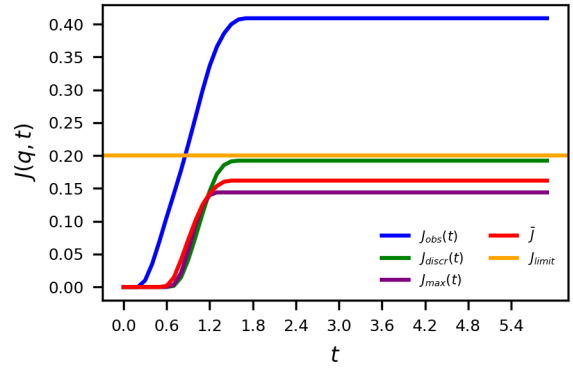
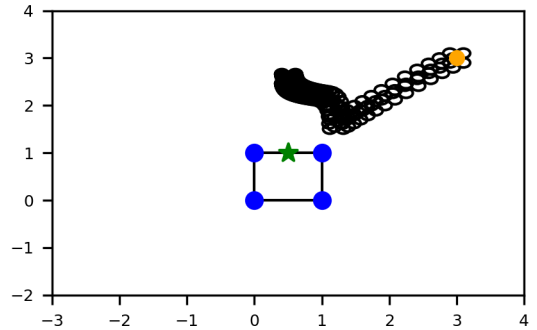
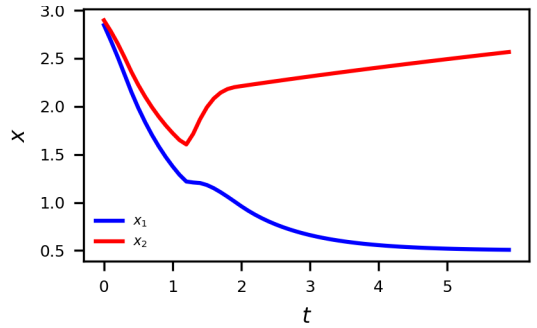


Fig. 2:  $J_{obs}(t)$ ,  $J_{discr}(t)$ ,  $J_{max}(t)$ ,  $\bar{J}$  and  $J_{limit}$  with time



(a) Goal at the obstacle



(b) Position at each time step

Fig. 3: Trajectory of the quadrotor when the goal is at the boundary of the obstacle

### E. Other parameters

We also ran the simulation with different parameters where  $A = 1.0$ ,  $\sigma = 0.55$  and the result can be seen in Fig. 1d which shows the quadrotor giving more safe distance away from the obstacle while heading towards the goal. This shows that by using a larger noise radius, the quadrotor adjusts its path to keep a wider distance from the obstacle as the noise radius increases. Finally, we ran a simulation with  $x_{goal} = [0, 5]$  near the obstacle, and from Figure 3a, it shows the quadrotor unable to get to the goal due to the accumulated noise at the obstacle which can be also seen in Figure 3b which shows the position of the robot at each time step and the plot shows the quadrotor bouncing back.

## VI. CONCLUSIONS

We presented a method to consider integral cost functionals into the framework of higher-order control barrier functions, enabling constraints over entire trajectories rather than just instantaneous states. Additionally, we present an efficient over-approximation method to handle constraints over large regions. Our simulations validate the ability of the agent (a simplified quadrotor) to navigate safely through environments while mitigating the impact of noise in sensitive areas. While we used acoustic noise emitted from quadrotors as an illustrative application, the theory we presented could be applied to other scenarios, such as managing light emission in microscopy or controlling vehicle pollution dispersion. Future research may extend this work to multi-agent systems, consider more accurate noise propagation and quadrotor dynamical models, and combine the our low-level control constraints into complete path planning solutions for cluttered environments.

## REFERENCES

- [1] A. D. Ames, J. W. Grizzle, and P. Tabuada. Control Barrier Function based quadratic programs with application to adaptive cruise control. In *53rd IEEE Conference on Decision and Control*, pages 6271–6278, 2014.
- [2] A. D. Ames, X. Xu, J. W. Grizzle, and P. Tabuada. Control barrier function based quadratic programs for safety critical systems. *IEEE Transactions on Automatic Control*, 62(8):3861–3876, 2017.
- [3] U. Borrmann, L. Wang, A. D. Ames, and M. Egerstedt. Control barrier certificates for safe swarm behavior. *IFAC-PapersOnLine*, 48(27):68–73, 2015.
- [4] T. H. Gronwall. Note on the derivatives with respect to a parameter of the solutions of a system of differential equations. *Ann. Math. (2)*, 20:292–296, 1919.
- [5] S. Karaman and E. Frazzoli. Sampling-based algorithms for optimal motion planning, 2011.
- [6] L. Lindemann and D. V. Dimarogonas. Control Barrier Functions for signal temporal logic tasks. *IEEE Control Systems Letters*, 3(1):96–101, 2019.
- [7] I. Tezuka and H. Nakamura. Safety assist control for nonautonomous control-affine systems via time-varying control barrier function. *IFAC-PapersOnLine*, 56(1):187–192, 2023. 12th IFAC Symposium on Nonlinear Control Systems NOLCOS 2022.
- [8] L. Wang, A. Ames, and M. Egerstedt. Safety barrier certificates for heterogeneous multi-robot systems. In *IEEE American Control Conference*, 2016.
- [9] L. Wang, A. D. Ames, and M. Egerstedt. Safety barrier certificates for collisions-free multirobot systems. *IEEE Transactions on Robotics*, 33(3):661–674, 2017.
- [10] G. Wu and K. Sreenath. Safety-critical and constrained geometric control synthesis using control lyapunov and control barrier functions for systems evolving on manifolds. In *IEEE American Control Conference*, pages 2038–2044. IEEE, 2015.
- [11] G. Wu and K. Sreenath. Safety-critical control of a planar quadrotor. In *IEEE American Control Conference*, pages 2252–2258. IEEE, 2016.
- [12] W. Xiao and C. Belta. Control Barrier Functions for systems with high relative degree. In *2019 IEEE 58th Conference on Decision and Control (CDC)*, pages 474–479, 2019.
- [13] G. Yang, C. Belta, and R. Tron. Continuous-time signal temporal logic planning with control barrier functions. In *2020 American Control Conference (ACC)*, pages 4612–4618, 2020.